Properties and Curing Kinetic of Diglycidyl Ether of Bisphenol A Cured with a Phosphorus-Containing Diamine

CHUN SHAN WANG, CHING HSUAN LIN

Department of Chemical Engineering, National Cheng Kung University, Tainan, Taiwan, Republic of China, 701

Received 21 December 1998; accepted 22 March 1999

ABSTRACT: Diglycidyl ether of bisphenol A (DGEBA) was cured with a new phosphorus-containing diamine, 1,4-bis(3-aminobenzoyloxy)-2-(6-oxido-6H-dibenz⟨c,e⟩⟨1,2⟩oxaphosphorin-6-yl)phenylene **II**, which was derived from 2-(6-oxido-6H-dibenz⟨c,e⟩⟨1,2⟩-oxaphosphorin-6-yl)-1,4-dihydroxy phenylene and 3-nitrobenzoyl chloride followed by hydrogenation. The structure of the synthesized phosphorus-containing curing agent **II** was confirmed through EA, IR, ^{1}H-NMR, and ^{31}P-NMR. The curing kinetics of the DGEBA/**II** system were studied by the dynamic and isothermal DSC method. Dynamic kinetic parameters were calculated by using the Kissinger and Ozawa's methods, respectively. Isothermal kinetic parameters, including k_1, k_2, m, and n, were determined by an autocatalytic mechanism proposed by Kamal. The model gives a good description of curing kinetics up to the onset of vitrification. The glass transition temperatures of cured epoxy (DGEBA/**II**) were 180°C based on DMA and 170°C by DSC, respectively. The onset decomposition temperatures (T_d onset) were 376 and 367°C under nitrogen and air, respectively. Char yields at 700°C were 38 and 18% under nitrogen and air, respectively. Limiting oxygen index (LOI) was 30, thus the phosphorus-containing diamine curing agent **II** was found to impart flame retardancy to the cured epoxy resin. © 1999 John Wiley & Sons, Inc. J Appl Polym Sci 74: 1635–1645, 1999

Key words: epoxy; flame retardancy; curing kinetics; LOI

INTRODUCTION

Epoxy resin is one of the most important products used widely in the polymer industry for coatings, adhesives, insulating materials, composites, etc. The diglycidyl ether of bisphenol A (DGEBA) has been the most important epoxy resin system in industry because of its fluidity, physical strength after curing, and cost advantage. Curing of the most commonly used epoxy resin, DGEBA, with a variety of aromatic diamines, was extensively reported in the literature.[1–3] However, these cured DGEBA systems cannot satisfy the applications that require flame retardancy.

Recently, many studies[4–9] on improving the flame retardancy of epoxy resins have been reported. However, the incorporation of bromide or phosphorus linkage into the polymer main chain results in the lowering of the thermal stability of epoxy and their degradation temperatures were lowered to around 200–300°C. This may be due to the presence of bromide or O═P—O in the polymer main chain reducing the thermal stability. Thus the flame retardancy was achieved by sacrificing thermal stability.

Kinetic characterization of thermoset resins is fundamental in understanding structure/property/processing relationships for manufacturing and utilization of high-performance composites. Differential scanning calorimetry (DSC) was used

Correspondence to: C. S. Wang.

Contract grant sponsor: National Science Council of Republic of China; contract grant number: NSC87-2622-E-006-005.

Journal of Applied Polymer Science, Vol. 74, 1635–1645 (1999)

 CCC 0021-8995/99/071635-11

extensively to characterize cure kinetics of thermosetting systems for a wide variety of applications regarding shelf-life predictions and optimization of processing conditions. Curing kinetics, curing rate, variation of rate at various temperatures, and activation energy are useful for the study of epoxy applications. These kinetic data provide information for the curing cycles of epoxies to ensure that the adequately cured epoxy is able to meet the requirements of its end use.

In this article, a phosphorus-containing diamine was synthesized and used to cure DGEBA. The diamine was characterized by FTIR, ^{1}H-NMR, and ^{31}P-NMR. The curing kinetics, flame retardancy, and thermal properties of cured epoxy were also evaluated by DSC, limiting oxygen index (LOI), thermogravimetric analyzer (TGA), and dynamic mechanical analyzer (DMA). Their properties were also compared with DGEBA/diamino diphenyl sulfone (DDS) system.

EXPERIMENTAL

Materials

2-(6-oxido-6H-dibenz⟨c,e⟩⟨1,2⟩oxaphosphorin-6-yl)-1,4-dihydroxy phenylene was synthesized in our laboratory according to the published procedure.[6] 3-nitrobenzoyl chloride, 4-nitrobenzoyl chloride (both from Acros), and 10% Pd/C (Ferak) were used without further purification. *N,N*-dimethylacetamide (Acros) was purified by distillation under reduced pressure over calcium hydride (Acros) and stored over 4 Å molecular sieves. Triethylamine (Ferak) was distilled before use. DGEBA with epoxy equivalent weight (EEW) 187 was supplied kindly by CCP in the Republic of China. 4,4′-DDS and 4,4′-diamino diphenyl methane (DDM) were purchased from Acros.

Characterization

DSC measurements were performed with a Perkin–Elmer DSC 7 supported by a Perkin–Elmer computer for data acquisition. The DSC was calibrated with high purity In and Zn. DSC dynamic data were obtained with 8 mg samples in a nitrogen atmosphere at a heating rate of 5–20°C/min by using a Perkin–Elmer DSC 7.

Isothermal cure reaction was conducted at five temperatures (130, 140, 150, 160, and 170°C). The reaction was considered complete when the isothermal DSC thermogram leveled off to the baseline. The total area under the exothermic curve, which was based on the extrapolated baseline at the end of the reaction, was used to calculate the isothermal heat of cure, ΔH_0. After the cure reaction was completed in the calorimeter, the sample was cooled to 40°C, and then, to determine the residual heat of reaction, ΔH_R, scanned at 10°C/min from 40 to 300°C. The sum of the isothermal (ΔH_0) and residual heat of the reaction (ΔH_R) was taken to represent the total heat of cure (ΔH_T). The isothermal conversion at time t was defined as $\alpha(t) = \Delta H_0/\Delta H_T$. TGAs were employed with a Perkin–Elmer TGA 7 at a heating rate of 5, 10, 20, 40°C/min under nitrogen or air from 60 to 700°C. The char yield is defined as the residual weight percent of polymer at 700°C on a TGA measurement. ^{1}H-NMR and ^{31}P-NMR spectra were obtained with a Bruker AMX-400 by using DMSO-d_6 as a solvent using tetramethylsilane (TMS) and H_3PO_4 as internal standards, respectively. The LOI was determined with an Atlas limiting oxygen index chamber according to the ASTM standard method. DMAs were made with a Perkin–Elmer DMA 7e. The storage modulus G' and tan δ were studied when the sample was subjected to a temperature scan mode at a programmed heating rate of 10°C/min from ambient to 220°C at a frequency of 1 Hz and an amplitude of 6 μm. A sample 15 mm in length, 10 mm in width and approximately 1.5 mm in thickness was used. The test method was performed by the three-point bending mode with a tension ratio at 110%.

Synthesis of Monomer

1,4-Bis(3-nitrobenzoyloxy)-2-(6-oxido-6H-dibenz-⟨c,e⟩⟨1,2⟩oxaphosphorin-6-yl) phenylene (I)

2-(6-oxido-6H-dibenz⟨c,e⟩⟨1,2⟩oxaphosphorin-6-yl)-1,4-dihydroxy phenylene (0.1 mol) dissolved in 200-ml dry THF, and triethylamine (0.22 mol) were introduced into a round-bottom 500-mL glass flask equipped with a nitrogen inlet, a condenser, and a mechanical stirrer (Scheme 1). After the reaction mixture was cooled to 10°C, 3-nitrobenzoyl chloride (0.22 mol) dissolved in 80 mL THF was added dropwise over 2 h. The reaction mixture was maintained at 20°C for another 2 h. The precipitate was filtered and recrystallized from glacial acetic acid and then dried in 100°C vacuum oven for 6 h. Yellow crystals (m.p. 236–237°C, 95% yield) of **I** were obtained. Mass [fastatom bombardment (FAB)] (*m/e*, relative intensi-

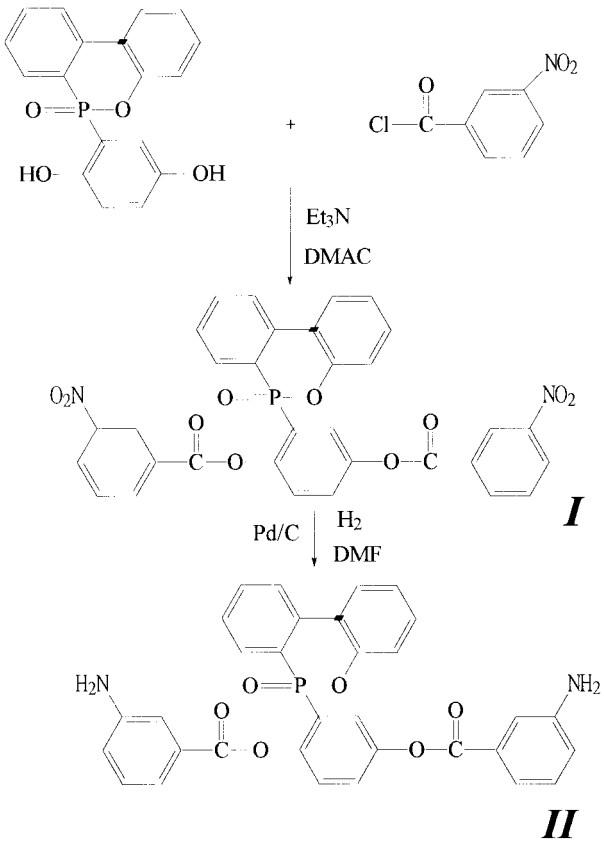

Scheme 1

ty): 623 (M + 1^+, 29.6), 154 (biphenyl, 100), 150 [(M − 472)$^+$ α cleavage of O═C—O, 29.2].

Elemental analysis for $C_{32}H_{19}O_{10}N_2P$ (622): Calcd. %: C, 61.74; H, 3.08; N, 4.50; Found %: C, 61.52; H, 3.09; N, 4.49. ^{1}H-NMR spectrum is 7.07 ppm (1H, *t*), 7.20 ppm (1H, *dd*), 7.22 ppm (1H, *t*), 7.53–7.64 ppm (5H, *m*), 7.75 ppm (1H, *d*), 7.80 ppm (1H, *d*), 7.88–7.96 ppm (4H, *m*), 8.21 ppm (1H, *dd*), 8.39 ppm (1H, *dd*), 8.59–8.61 ppm (2H, *m*), and 8.86 ppm (1H, *t*). ^{31}P-NMR spectrum: 15.18 ppm (*s*).

1,4-Bis(3-aminobenzoyloxy)-2-(6-oxido-6H-dibenz-⟨c,e⟩⟨1,2⟩oxaphosphorin-6-yl) phenylene (II)

The dinitro compound (**I**) 6 g, 0.1 g of 10% Pd/C, and 50 ml of DMF were introduced into a miniclave (a glass pressure reactor, Buchiglasuster, Switzerland) at room temperature. The miniclave was placed on a magnetic stirrer to agitate the contents. The reaction system was purged with nitrogen for 1 min before the hydrogen addition, and the pressure was kept at about 7 kg/cm^2 under hydrogen for 8 h. The reaction mixture was then filtered to remove Pd/C. The filtrate thus obtained was poured into 500 mL of stirring water, giving rise to a precipitate that was isolated by filtration. White crystals (m.p. 214–215°C, 98% yield) of **II** were obtained.

Mass (FAB) (*m/e*, relative intensity): 563 (M + 1^+, 3.6), 120 [(M − 446)$^+$ α cleavage of O═C—O, 100]. Elemental analysis for $C_{32}H_{23}O_6N_2P$ (562): Calcd. %: C, 68.31; H, 4.12; N, 4.98; Found %: C, 68.11; H, 4.18; N, 5.08. ^{1}H-NMR spectrum is 5.16 ppm (2H, —NH_2, *s*), 5.50 ppm (2H, —NH_2, *s*), 6.38 ppm (1H, *d*), 6.70–6.78 ppm (5H, *m*), 7.19–7.51 ppm (8H, *m*), 7.69–8.04 ppm (5H, *m*). ^{31}P-NMR spectrum: 16.91 ppm (*s*).

Preparation of Polymers

The cured epoxy (code number: DGEBA/**II**) and control epoxy (code number: DGEBA/DDS and DGEBA/DDM) were obtained via thermal curing. The reactants (DGEBA and **II** or DDS or DDM) were mixed homogeneously at a 1 : 1 equivalent ratio. The curing condition was 150°C for 1 h, then 180°C for 4 h.

RESULTS AND DISCUSSION

Synthesis of *II*

1,4-Bis(3-nitrobenzoyloxy)-2-(6-oxido-6H-dibenz-⟨c,e⟩⟨1,2⟩oxaphosphorin-6-yl) phenylene (**I**) was synthesized from 2-(6-oxido-6H-dibenz⟨c,e⟩⟨1,2⟩-oxaphosphorin-6-yl)-1,4-dihydroxy phenylene and 3-nitrobenzoyl chloride at low temperatures. The reaction took place as soon as 3-nitrobenzoyl chloride was introduced at 20°C because white $Et_3N^{\bullet}HCl$ was observed immediately after the addition of 3-nitrobenzoyl chloride.

Reduction of the dinitro compound to an amino compound can be carried out in a number of ways [e.g., the catalytic hydrogenation (H_2/Pd–C), acid (HCl), and metal or metal salt, or hydrazine hydrate/Pd-C]. In the present work, the dinitro compound **I** was catalytically hydrogenated with Pd/C because this method led to higher yields than the corresponding reduction carried out with hydrazine hydrate and also did not cleave the ester group of the dinitro compound **I** during reduction. (When hydrazine hydrate/Pd-C was used to reduce **I**, a single crystal with a very sharp melting point of 231°C was observed by DSC scan; however, no elemental phosphorus was detected by X-ray single crystal diffraction or by ^{31}P-NMR spectrum. Thus we concluded that the ester group was cleaved.) **II** shows characteristic bands in the

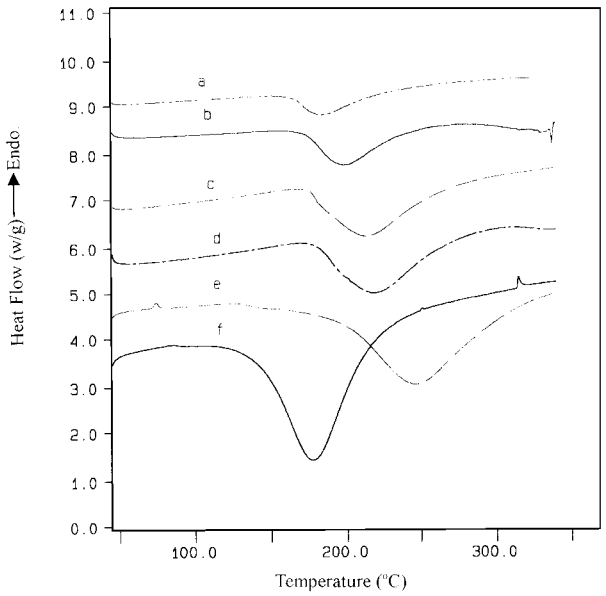

Figure 1 DSC traces of DGEBA/**II** system at various heating rates. (a) 5, (b) 10, (c) 15, and (d) 20°C/min, (e) DGEBA/DDS at a heating rate of 20°C/min, and (f) DGEBA/DDM at a heating rate of 20°C/min.

IR spectrum [i.e., 924(P—O—Ar), 1179(P—O—Ar), 1212(Ar—O), 1461(P—Ar), 1738(C═O), 3047(Aromatic H), 3478, 3440, 3376, 3328 (NH_2)]. Chemical shift and splitting pattern of ^{1}H-NMR spectrum of **II** is 5.16 ppm (2H, —NH_2, *s*), 5.50 ppm (2H, —NH_2, *s*), 6.38 ppm (1H, *d*), 6.70–6.78 ppm (5H, *m*), 7.19–7.51 ppm (8H, *m*), 7.69–8.04 ppm (5H, *m*). ^{31}P peak: 16.91 ppm (*s*). Owing to the coupling effect (*ortho, meta* of aromatic ring, and P—H coupling), no attempt was made to assign each ^{1}H peak in **I** and **II**; however, the integral areas correspond to the structures. The elemental analysis, mass spectrometric analysis, characteristic peaks in the ^{1}H-NMR, and ^{31}P-NMR spectra and characteristic bands in the IR spectra correlate sufficiently well with the proposed structures.

Curing Behaviors

The curing behaviors of DGEBA/**II**, DGEBA/DDS, and DGEBA/DDM systems were studied by dynamic DSC heating scans and the results are shown in Figure 1. Figure 1(d)–(f) shows the DSC thermograms of DGEBA/**II**, DGEBA/DDS, and DGEBA/DDM at a heating rate of 20°C/min, respectively. The exothermic peak temperatures for Figure 1(d)–(f) are 220, 247, and 178°C, respectively. A curing agent, exhibiting a lower peak exothermic temperature under the same set of curing conditions, is more reactive toward the epoxy resins. It is, therefore, reasonable to propose that the chemical reactivity of these three curing agents toward the epoxy resin is DDS < **II** < DDM. The sulfone group is a strong electron withdrawing group both by induction ($-I$) and mesomeric ($-M$) effects. Because the nucleophilic amino groups are located in the *para* position for DDS, its nucleophilicity is considerably reduced. The mesomeric effect ($-M$) of DDS is shown as follows.

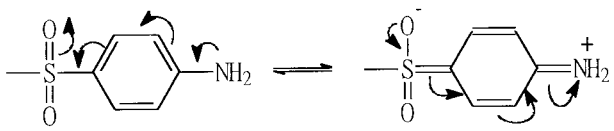

Although ester groups in **II** also have $-I$ effects, the $-M$ effect is less for **II** because the amino group is in the *meta* position and the amino group cannot resonate with the C═O group. Its resonance condition is shown as follows.

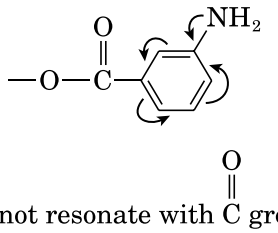

Since the amino group cannot resonate with the C═O group, the decreased nucleophilicity of **II** by the mesomeric effect is less than that of DDS. The inductive effect ($-I$) in the *meta* position will be stronger than in the *para* position. However, the two effects compensate for each other and result in similar starting exothermic temperatures for the two curing agents (**II** and DDS). According to organic chemistry, the influence of the mesomeric effect is stronger than the inductive effect, thus **II** has a lower exothermic peak temperature (higher reactivity than that of DDS). DDM, with positive inductive effect ($+I$) but no mesomeric effect by the methyl group, is thus more reactive than DDS and **II**.

Curing Kinetics

Dynamic Method I (Kissinger's Method[10])

The data from dynamic DSC measurements are analyzed by

$$r = \frac{dx}{dt} = \beta\frac{dx}{dt} = Ae^{(E/RT)}(1-x)^n \qquad (1)$$

Because the maximum rate takes place when dr/dt is zero, differentiating eq. (1) with respect to time and equating the resulting expression with zero gives

$$\beta\frac{E}{RT_p^2} = An(1-x)p^{n-1}e^{(-E/RT_p)} \qquad (2)$$

where T_p is the maximum rate temperature. Equation (2) can be written in the natural logarithm form shown in eq. (3)

$$-\ln\left(\frac{\beta}{T_p^2}\right) = \ln\left(\frac{E}{R}\right) - \ln(An) - (n-1)\ln(1-x)_p + \frac{E}{RT_p} \qquad (3)$$

Figure 1(a)–(d) shows the heating scans of DGEBA/**II** under various heating rates. From the peak temperature and heating rate, we can get the data for the plot of ln (β/T_p^2) against $(1/T_p)$, and a linear plot of $-\ln(\beta/T_p^2)$ versus $(1/T_p)$ as shown in Figure 2(a). The activation energy can be obtained from the slope of the corresponding straight line. The activation energy calculated from Figure 2(a) is 58.3 kJ/mol.

Dynamic Method II (Ozawa's Method[11])

Another theoretical treatment, namely Ozawa's method, can also be applied to the thermal data. He reported

$$\log\beta = \frac{1}{2.303}\ln\beta = -0.4567\frac{E}{RT} + \left(\log\frac{AE}{R} - \log F(x) - 2.315\right) \qquad (4)$$

where β is the heating rate, E is the activation energy, R is the ideal gas constant, and $F(X)$ is the conversion-dependent term.

Thus, at the same conversion, a plot of ln(β) versus $1/T_p$ [Fig. 2(b)] should be a straight line with a slope of $(2.303 \times 0.4567)E/R$. The activation energy calculated from Figure 2(b) is 62.9 kJ/mol.

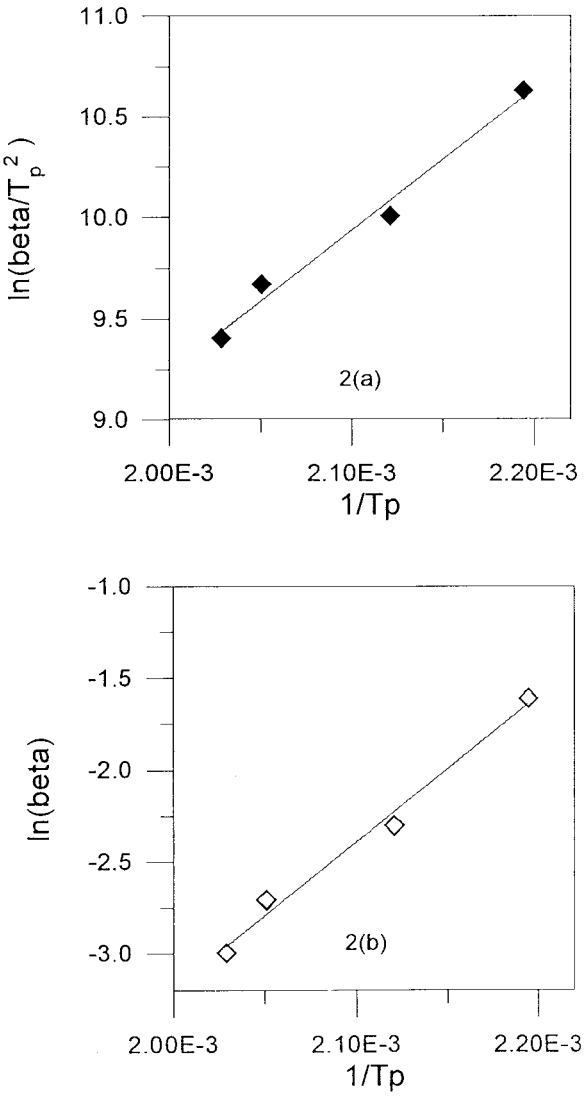

Figure 2 (a) Plot of $-\ln(\beta/T_p^2)$ versus $1/T_p$, (b) plot of ln (β) versus $1/T_p$.

Isothermal Curing Kinetics (Kamal's Equation[12])

A conventional model of the autocatalytic curing reaction was assumed and investigated. Generally, most amine-cured epoxy systems are expressed as follows:

$$d\alpha/dt = (k_1 + k_2\alpha^m)(1-\alpha)^n \qquad (5)$$

where α is the conversion, k_1 and k_2 are the apparent rate constants, and m and n are the kinetic exponents of the reactions. The constant k_1 in this equation can be calculated from the initial reaction rate at $\alpha = 0$. The kinetic constants are assumed to be of the Arrhenius form k_1

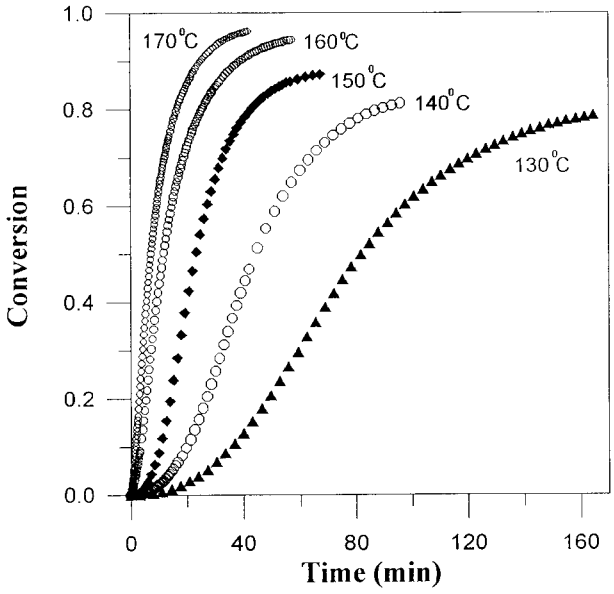

Figure 3 Plots of conversion (α) against cure time for DGEBA/**II** blend at various temperatures (130, 140, 150, 160, and 170°C, respectively).

$= A_1\exp(-E_1/RT)$ and $k_2 = A_2\exp(-E_2/RT)$, where A_1, A_2 are the preexponential constant, E_1, E_2 are the activation energy, R is the gas constant, and T is absolute temperature. Equation (5) is rewritten in the following form:

$$\ln(d\alpha/dt) = \ln(k_1 + k_2\alpha^m) + n\ \ln(1 - \alpha) \quad (6)$$

Except for the initial region, a plot of $\ln(d\alpha/dt)$ versus $\ln(1 - \alpha)$ is expected to be linear with a slope n. Equation (6) can then be further rearranged to give

$$\ln\{[(d\alpha/dt)/(1 - \alpha)^n] - k_1\} = \ln k_2 + m\ \ln \alpha \quad (7)$$

The first term of eq. (7) can be computed from the previously estimated values of k_1 and n. If the left term of eq. (7) is plotted against $\ln(\alpha)$, a straight line is yielded, the slope and intercept of which allow the estimation of m and kinetic constant k_2, respectively. Preliminary kinetic parameters can be obtained on the first trial. The kinetic parameters, k_2, m, and n can be estimated from the stated procedures. To obtain a more precise value, an iterative procedure should be utilized. The equation can be further rearranged to give the following form:

$$\ln(d\alpha/dt) - \ln(k_1 + k_2\alpha^m) = n\ \ln(1 - \alpha) \quad (8)$$

The left terms of the above equation can be plotted against $\ln(1 - \alpha)$. A new value of the reaction order n can be obtained from the slope. The same iterative procedure can be repeated until apparent convergence of m and n values.

A plot of conversion against cure time for DGEBA/**II** system at various temperatures is shown in Figure 3. At a given time, the degree of conversion increases with increasing cure temperature. Figure 4 shows the plot of $d\alpha/dt$ versus time at various temperatures. It is seen that the reaction rate is affected by the isothermal curing temperature and reaction time. At a given temperature, the reaction rate is observed to increase initially with conversion and passes through a maximum, and then gradually slows down, finally tending to zero. Additionally, at a given time, a higher isothermal curing temperature gains a higher reaction rate. Moreover, the higher the isothermal temperature, the shorter the reaction time. Figure 4 shows that the reaction rate of the system reaches a maximum at time $t > 0$, which is characteristic of an autocatalytic reaction, so the autocatalytic kinetic model is appropriate to describe the isothermal behavior of the system. The values of m and n obtained for each curing temperature are shown in Table I. Rate constants k_1 and k_2 are shown as an Arrhenius plot in Figure 5, which yields the value of 147 and 46 kJ/mol for the associated activation energies (E_1 and E_2). In an ideal condition, a successful model

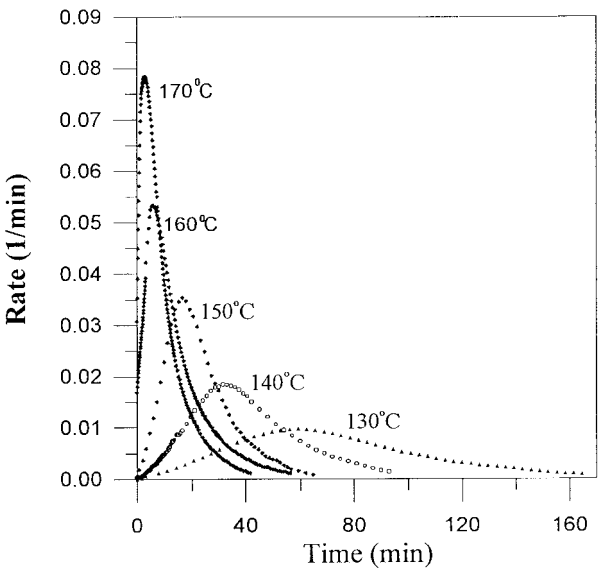

Figure 4 Plots of $d\alpha/dt$ versus time plot for DGEBA/**II** blend at different temperatures (130, 140, 150, 160, and 170°C, respectively).

Table I Values of *m* and *n* Estimated at Different Temperatures

Temperature (°C)	*m*	*n*
130	0.93	2.33
140	0.83	2.10
150	0.82	1.99
160	0.77	1.78
170	0.48	1.51

should describe the experimental data well throughout the whole range of cure. But in this work, the diffusion and etherification reaction were not taken into account in the kinetic model. To demonstrate the curing behavior described by the Kamal equation, it is necessary to compare the results from model prediction with the experimental data. Figure 6 is the $d\alpha/dt$ versus α plot at various temperatures. The autocatalytic model (solid line in Fig. 6) fits the experimental data quite well in the early stage of the curing. However, deviations are observed in the later stage, which are attributed to the effect of diffusion.

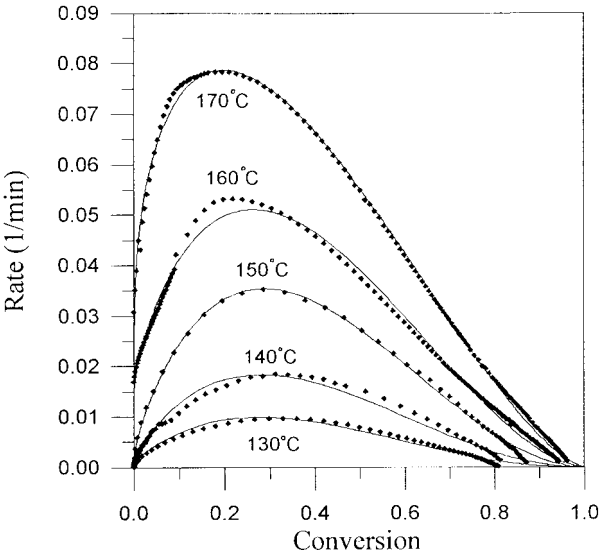

Figure 6 Plots of $d\alpha/dt$ versus α at different temperatures (130, 140, 150, 160, and 170°C, respectively) (◆) is experimental data and solid line is autocatalytic model).

Thermal Properties of Cured Epoxy Resins

TGA Analysis. TGA traces of phosphorus-containing epoxy resin provided additional information regarding their thermal stability and thermal degradation behavior. TGA curves and first derivative of TGA curves of cured epoxy (DGEBA/**II**) and control epoxy (DGEBA/DDS) under nitrogen and air are shown in Figure 7(a) and (b). Although the onset degradation (T_d onset) and maximum decomposition (T_d max) temperatures for DGEBA/**II** are slightly lower than DGEBA/DDS, however, T_d onset of DBEGA-**II** (376°C under nitrogen and 367°C under air) is higher than other phosphorus-containing epoxy.[5] TGA traces of the epoxy in air revealed two decomposition steps because of the oxidative degradation of the carbonaceous residue. Van Krevelen[13] has proposed that the char residue on pyrolysis is linearly proportional to the oxygen index of halogen-free polymers. Increasing char formation can limit the production of combustible gases, decrease the exothermicity of the pyrolysis reaction, and decrease the thermal conductivity of the burning materials, and consequently, limit the flammability of the materials. Compared with phosphorus-free epoxy (DGEBA/DDS and DGEBA/DDM), the char yield of DGEBA/**II** at 700°C under nitrogen was 32%, whereas the DGEBA/DDS was 15% and DGEBA/DDM was 13%, so the char yield-enriching effect of phosphorus element was demonstrated. Although the char yields of phosphorus-free epoxy at 700°C under air was <1%, the char yield of phosphorus-containing epoxy was about 18%. These high char yields imply that the flame retardancy of the epoxy resins was elevated by using the phosphorus-containing diamine as a curing agent. This result was further confirmed by the LOI measure-

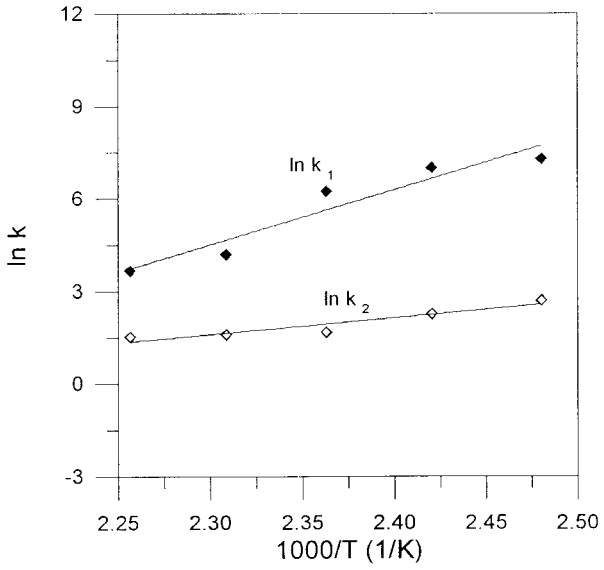

Figure 5 Arrhenius plot of rate constants k_1 and k_2.

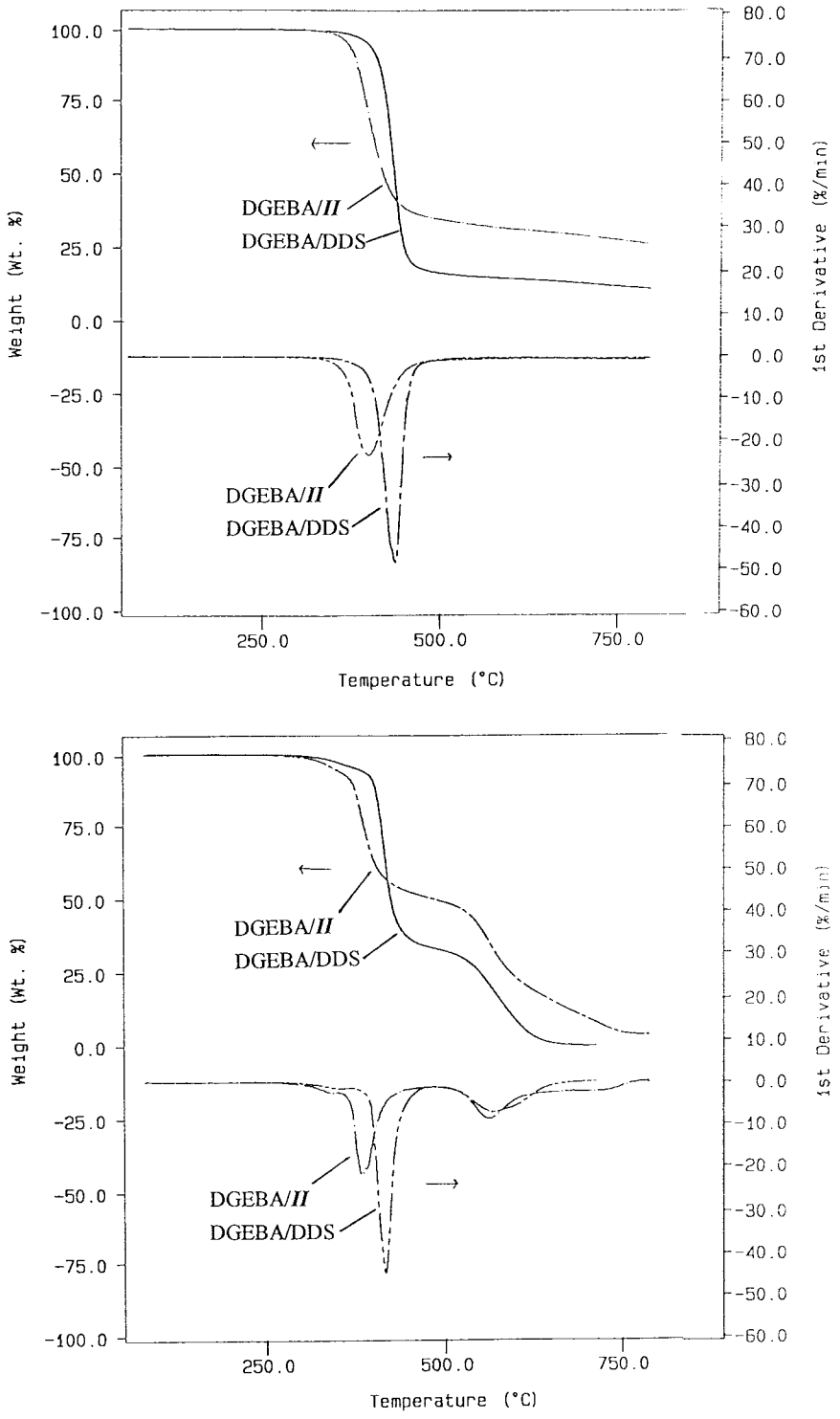

Figure 7 TGA curves and first derivative of TGA curves of DGEBA/**II** and DGEBA/DDS (a) under nitrogen, (b) under air.

ment. LOI is defined as the minimum fraction of oxygen in an oxygen–nitrogen mixture that is just sufficient to sustain combustion of the specimen after ignition. Compared with the LOI of DGEBA/DDS (LOI = 22) and DGEBA/DDM (LOI = 21), the LOI of DGEBA/**II** (LOI = 30) implies that the flame

retardancy of epoxy was improved via the incorporation of phosphorus element. These results are consistent with the TGA results.

Activation Energy of Degradation

The activation energy was determined by Ozawa's method[11] described in the dynamic curing kinetic section. This practical approach in evaluating thermal resistance and thermal degradation was also applied to a variety of commercial aromatic polymers[14] including polyimides, poly(etherimide), poly(ether sulfone), poly(aryl ether ether ketone), and poly(*p*-xylylene).

Figure 8(a) and (b) shows decomposition profiles of DGEBA/**II** at various heating rates ($\sim$ 5–40°C/min) under nitrogen or air, respectively. As can be seen in Figure 8(a), TGA curves at various heating rates are parallel to one another; therefore, the thermal decomposition of the epoxy (DGEBA/**II**) in nitrogen was controlled by a single activation energy. However, the thermal decomposition under air is more complex than that under nitrogen, so the activation energy can be calculated only before decomposition conversion is $<$30%. The ln(β) versus T^{-1} plot of DGEBA/**II** at several decomposition conversions according to eq. (4) is shown in Figure 9(a) and (b), respectively. Straight lines were drawn according to the method of least squares. From these lines, the degradation activation energies of DGEBA/**II** at various conversions under nitrogen and air are determined and shown in Figure 10. To our surprise, the degradation activation energy of DGEBA/**II** under air was higher than that under nitrogen. The results shown in Figure 10 indicated that the phosphorus group might react with air and formed a protective char layer, which increased the degradation activation energies drastically under air.

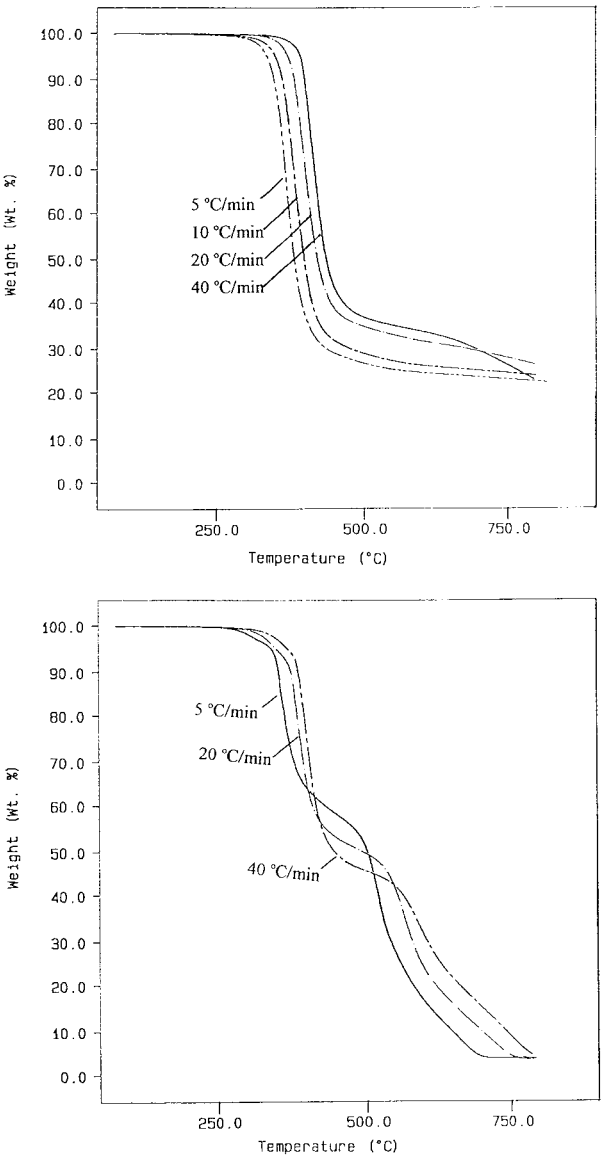

Figure 8 Decomposition profiles of DGEBA/**II** at various heating rate (5°C/min $\sim$ 40°C/min) under (a) under nitrogen, (b) under air.

DMA Analysis

More detailed information may be obtained from measurements of the dynamic mechanical behavior of the samples as a function of temperature. Figure 11 shows the DMA curves of the cured epoxy (DGEBA/**II**) and control epoxy (DGEBA/DDS) at a heating rate of 10°C/min from 0 to 220°C. Both epoxys show similar dynamic mechanical behavior (G' and tan δ) by DMA. However, DGEBA/**II** has retained less (lower) modulus at high temperature than DEGBA/DDS; this implies that DGEBA/**II** has less crosslink density than DGEBA/DDS. This is consistent with the structure of **II** being a larger molecule than that of DDS, which results in a longer distance between the two crosslink points. The main transition at around 180°C is associated with an approximately 2 order of magnitude decrease in G'. This transition could be indicative of a glass transition. Moreover, DSC showed an endothermic transition at 170°C, a fact that supports the glass transition temperature. DGEBA/**II** exhibited a high initial G' value ($\sim 10^9$ Pa) and about 10^9 Pa up to 180°C. DMA analysis shown in Figure 11

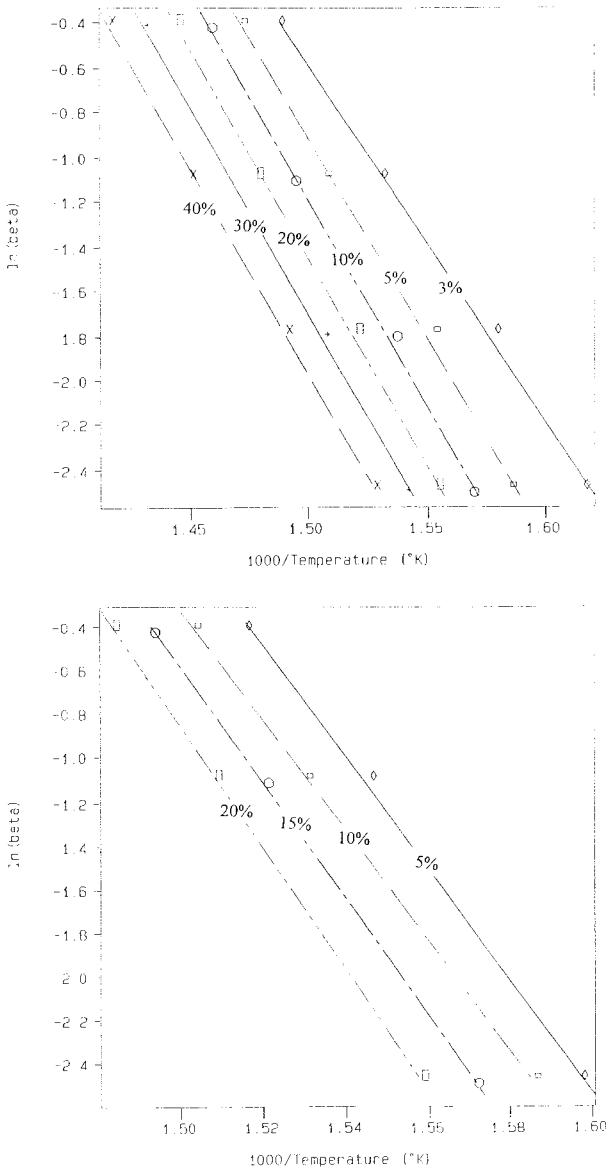

Figure 9 The ln (β) versus T^{-1} plot of DGEBA/**II** at several decomposition conversions, (a) under nitrogen, (b) under air.

displayed a β relaxation at about 50–80°C for DGEBA/**II**, which is not observed in the DGEBA/DDS system. A transition at 50–80°C was assigned to the mobility of the side chain accompanied by some conformational rearrangements of the main chain.[15–16]

CONCLUSION

A phosphorus-containing diamine **II** was prepared and used to cure DGEBA. The structure of

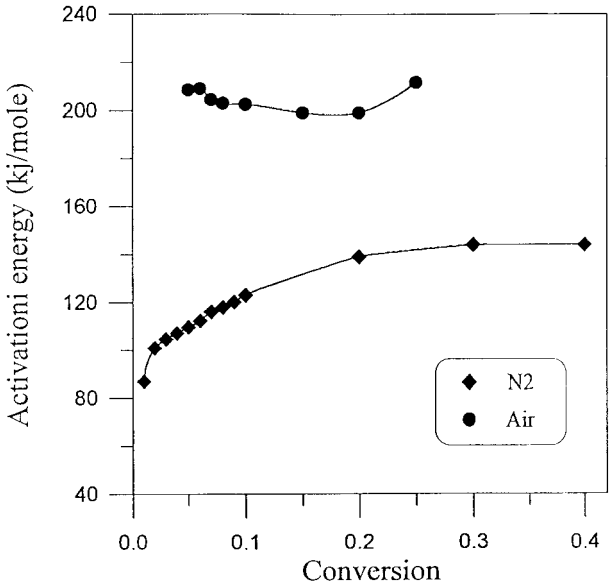

Figure 10 The degradation activation energies of DGEBA/**II** at various conversions under nitrogen and air.

II was confirmed through EA, IR, ^{1}H-NMR, and ^{31}P-NMR. The curing kinetics of DGEBA/**II** were studied by the Kissinger, Ozawa, and Kamal's methods. The Kamal's model gives a good description of curing kinetic up to the onset of vitrification. The glass transition temperature of cured epoxy (DGEBA/**II**) was about 180°C based on DMA and 170°C by DSC. DGEBA/**II** exhibits high thermal stability and flame retardancy.

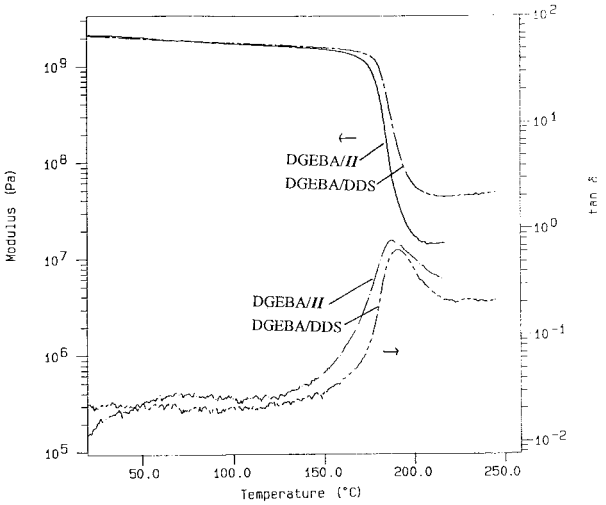

Figure 11 Dynamic mechanical analyses curves of DGEBA/**II** and DGEBA/DDS at a heating rate of 10°C/min.

Financial support of this work by the National Science Council of Republic of China is gratefully appreciated (NSC87-2622-E-006-005).

REFERENCES

1. Bennett, G. S.; Farris, R. J.; Thompson, S. A. Polymer 1991, 32, 1633.
2. Kinloch, A. J.; Shaw, S. J.; Tod, D. A.; Hunston, D. L. Polymer 1993, 24, 1341.
3. Gupta, N.; Varma, I. K. J Appl Polym Sci 1998, 68, 1759.
4. Mikroyannidis, J. A.; Kourtides, D. A. J Appl Polym Sci 1984, 29, 197.
5. Lewis, M.; Atlas, S. M.; Pearce, E. H. Flame Retardant Polymeric Materials; Plenum: New York, 1975.
6. Chin, W. K.; Hsau, M. D.; Tsai, W. C. J Polym Sci, Polym Chem 1995, 33, 373.
7. Liu, Y. L.; Hsiue, G. H.; Lee, R. H.; Chiu, S. Y. J Appl Polym Sci 1997, 63, 895.
8. Liu, Y. L.; Hsiue, G. H.; Chiu, Y. S.; Jeng, R. J.; Perng, L. H. J Appl Polym Sci 1996, 61, 613.
9. Wang, T. S.; Shau, M. D. J Appl Polym Sci 1998, 70, 1877.
10. Kissinger, H. E. Anal Chem 1957, 29, 1072.
11. Ozawa, T. Bull Chem Soc Jpn 1965, 38, 1881.
12. Kamal, M. R. Polym Eng Sci 1974, 14, 23.
13. Van Krevelen, D. W. Polymer 1975, 16, 615.
14. Chiu, J. in Polymer Characterization by Thermal Methods of Analysis, Marcel Dekker: New York, 1974; p 157.
15. Kallitsis, J.; Gravalos, K.; Dondos, A. Macromolecules 1993, 26, 5457.
16. Frosini, V.; Butta, E. J Polym Sci, Polym Lett Ed 1967, 9, 253.